

Inhomogeneity and glass-forming ability in the bulk metallic glass $\text{Pd}_{42.5}\text{Ni}_{7.5}\text{Cu}_{30}\text{P}_{20}$ as seen via x-ray spectroscopies

S. Hosokawa,^{1,2,*} H. Sato,³ T. Ichitsubo,⁴ M. Nakatake,³ N. Happo,⁵ J.-F. Bérar,⁶ N. Boudet,⁶ T. Usuki,⁷ W.-C. Pilgrim,² E. Matsubara,⁴ and N. Nishiyama⁸

¹Center for Materials Research Using Third-Generation Synchrotron Radiation Facilities, Hiroshima Institute of Technology, Hiroshima 731-5193, Japan

²Physikalische Chemie, Fachbereich Chemie, Philipps Universität Marburg, D-35032 Marburg, Germany

³Hiroshima Synchrotron Radiation Center, Hiroshima University, Higashi-Hiroshima 739-0046, Japan

⁴Department of Materials Science and Engineering, Graduate School of Engineering, Kyoto University, Kyoto 606-8501, Japan

⁵Graduate School of Information Sciences, Hiroshima City University, Hiroshima 731-3194, Japan

⁶Institut Néel, CNRS, F-38042 Grenoble Cedex, France

⁷Department of Material and Biological Chemistry, Faculty of Science, Yamagata University, Yamagata 990-8560, Japan

⁸R&D Institute of Metals and Composites for Future Industries, Sendai 980-8577, Japan

(Received 2 May 2009; revised manuscript received 10 September 2009; published 17 November 2009)

Core-level photoemission spectroscopy and anomalous x-ray scattering (AXS) measurements were performed for the $\text{Pd}_{42.5}\text{Ni}_{7.5}\text{Cu}_{30}\text{P}_{20}$ (PNCP) excellent metallic glass to investigate the chemical nature and local atomic structure, and the results were compared to those in $\text{Pd}_{40}\text{Ni}_{40}\text{P}_{20}$ and $\text{Pd}_{40}\text{Cu}_{40}\text{P}_{20}$. The P $2p$ core levels clearly separate into two states, indicating that the P atoms have two different chemical sites, which is a strong experimental proof for the existence of an elastic inhomogeneity. From the AXS close to the Pd K edge, a specific Pd-P-Pd atomic configuration was observed, which is related to the stable state in the P $2p$ core levels. All of the core levels measured in PNCP have the deepest binding energies among these glasses, indicating the most stable electronic states. Local structure around the P atoms is discussed by the AXS data and a metastable crystal appeared in a supercooled metallic alloy close to PNCP.

DOI: [10.1103/PhysRevB.80.174204](https://doi.org/10.1103/PhysRevB.80.174204)

PACS number(s): 81.05.Kf, 61.05.cp, 71.23.Cq

I. INTRODUCTION

Disordered materials exhibit complex relaxation processes,¹ and the correlation between these dynamic processes and the glass structure is one of the main issues in glass science. One focus has been the tendency of the high-frequency acoustic modes to disperse faster than expected from measurements of the ultrasonic sound velocity. This positive dispersion is frequently observed in many disordered systems.² For liquids, the positive dispersion may be explained within the framework of generalized hydrodynamics³ or mode-coupling theory.⁴ However, positive dispersion is also observed in glasses, e.g., silica glass^{5,6} and the phenomenon has been attributed to a residual fast process in the glass.⁶

Ichitsubo *et al.*⁷ have recently carried out inelastic x-ray scattering (IXS) measurements on $\text{Pd}_{42.5}\text{Ni}_{7.5}\text{Cu}_{30}\text{P}_{20}$ (PNCP). They also performed ultrasonic measurements to determine the elastic moduli at low temperatures,⁸ where any residual processes in the glass should have been frozen out. In those works, they have experimentally shown that the sound velocity of the nanometer-wavelength acoustic phonons exceeds that of millimeter wavelengths (the ultrasound velocity on the macroscopic scale) in this glass, when the glass is completely frozen far below the glass transition temperature. This can be viewed as an evidence that nano-scale elastically harder regions exist in the glass matrix, and hence, elastically softer regions should also be present so as to realize the macroscopic elasticity.⁹ Theoretical evidence for the elastic inhomogeneity was already given by Schirmacher *et al.*^{10,11} However, experimental evidence has not yet

been obtained in static points of view, such as atomic structure or electronic properties.

In another viewpoint of glass-forming ability (GFA), PNCP discovered in 1996 by Nishiyama and Inoue¹² has at present the lowest critical-cooling-rate (CCR) value of 0.067 K/s and can form a massive bulk glass with a diameter of more than 40 mm.¹³ On the contrary, its underlying alloy $\text{Pd}_{40}\text{Ni}_{40}\text{P}_{20}$ (PNP) has a worse CCR of about 2 K/s (Ref. 14) and $\text{Pd}_{40}\text{Cu}_{40}\text{P}_{20}$ (PCP) shows a much worse CCR of more than 10^3 K/s. Experimental attempts have not been performed in the microscopic sense in detail, and thus, the origin of the excellent GFA in this glass has not yet been well understood.

In this paper, we present results of core-level photoemission spectroscopy (PES) and anomalous x-ray scattering (AXS) on these typical bulk metallic glasses (BMGs). From the determination of the chemical nature and the local structure of the constituent elements, we have found a firm evidence for the existence of microscopic inhomogeneity appearing on the P sites, which may be related to the excellent GFA of the PNCP metallic glass. We also found a special Pd-P-Pd configuration from the AXS experiment, which may act as a high stability against the crystallization.

The paper is organized as follows. In Sec. II, we briefly describe experimental procedure of the core-level PES and AXS measurements. Section III gives the results obtained, and in Sec. IV, we discuss the local structure and the chemical nature in relation to the inhomogeneity and excellent GFA in the PNCP metallic glass. Finally, we sum up our present results.

TABLE I. The large contributions of $S_{ij}(Q)$ (more than 0.05) to the $\Delta_{\text{Pd}}S(Q)$ and $S(Q)$ in the $\text{Pd}_{42.5}\text{Ni}_{7.5}\text{Cu}_{30}\text{P}_{20}$ alloy at the first maximum in $S(Q)$ at about 29 nm^{-1} .

	Pd-Pd	Pd-Cu	Pd-P	Pd-Ni	Cu-Cu
$S(Q)$	0.38	0.31	0.10	0.07	0.06
$\Delta_{\text{Pd}}S(Q)$	0.56	0.29	0.08	0.07	(0)

II. EXPERIMENTAL PROCEDURE

The PNCP and PNP rods with a diameter of 3 mm were prepared as follows. Prior to making the master ingots, a Pd-P prealloy was prepared using Pd and P polycrystals with the purities of 99.95% and 99.9999%, respectively. Then, master ingots were made by arc-melting mixtures of pure Pd, Ni, Cu, and the prealloyed Pd-P in an Ar atmosphere. The purities of Ni and Cu were 99.9% and 99.99%, respectively. In order to eliminate heterogeneous nucleation due to oxide contamination, a B_2O_3 flux treatment¹⁴ was repeatedly (typically ten times) carried out in a highly purified Ar atmosphere with an O_2 content of less than 10 ppm. The melts were kept at about 1273 K for at least six days and then quenched into iced water. The details of the sample preparation are given elsewhere.¹³ The PCP sample was prepared from the melts using a rapid quenching technique. The absence of crystallinity in the samples was confirmed by x-ray diffraction and calorimetry. Sample composition was checked to be within 1% by electron-probe microanalysis both before and after the experiments.

The core-level PES spectra were measured using a spectrometer at the beamline BL7 of Hiroshima Synchrotron Radiation Center. Vacuum-ultraviolet photons generated from the storage ring HiSOR with a ring energy of 700 MeV and a ring current of 160–300 mA were monochromatized with a Dragon-type monochromator covering incident photon energy values, $h\nu$, from 20 to 380 eV. A PES spectrometer with a hemispherical photoelectron energy analyzer (GAMMA-DATA SCIENTA SES2002) attached to the analyzer chamber at the end station of BL7 was used for the core-level PES experiments. The overall energy resolution of the PES spectrometer was set to be about 0.10 eV at $h\nu=220 \text{ eV}$ for the Ni $3p$, Cu $3p$, and P $2p$ spectra, and about 0.53 eV at $h\nu=450 \text{ eV}$ for the Pd $3d$ spectra. The details of the setup are given elsewhere.¹⁵

All of the core-level PES spectra were collected at room temperature. Clean surfaces were obtained by sputtering the samples with Ar^+ ions in a sample preparation chamber with the base pressure below 1×10^{-10} mbar. No core spectra due to oxygen or carbon contamination were visible within 24 h after the sample surface cleaning, and the measurements were performed within 12 h. The energies of all spectra were defined with respect to the Fermi energy E_F of the sample or a freshly prepared Au film.

The AXS experiments were carried out at the beamline BM02 of the European Synchrotron Radiation Facility (ESRF). For obtaining the differential structure factors, $\Delta_i S(Q)$, around the Pd, Ni, and Cu atoms, two x-ray scattering experiments were performed in a reflection geometry at incident x-ray energies below each K absorption edge, i.e.,

30 eV below the Pd K edge (24350 eV) or 20 eV below the Ni K (8333 eV) and Cu K (8979 eV) edges, and 200 eV below each K edges, using a standard $\omega-2\theta$ diffractometer installed at the beamline. Due to the high energy of the Pd K edge, the measurable Q range was up to 180 nm^{-1} , which is very effective to suppress the truncation errors on calculating the pair distribution functions, $g(r)$. The experimental setup, in particular, the new detecting system using a graphite analyzer crystal, is given in detail elsewhere.¹⁶

Following the analyzing procedure given in Ref. 17, the $\Delta_i S(Q)$ close to the respective absorption edges were calculated from each pair of the scattering data. For each $\Delta_i S(Q)$, the corresponding i th-edge-element-related partial structure factors, $S_{ij}(Q)$, dominate $\Delta_i S(Q)$. For example, Table I shows the large contributions of $S_{ij}(Q)$ (more than 0.05) to the $\Delta_{\text{Pd}}S(Q)$ and $S(Q)$ of the PNCP alloy at the first maximum in $S(Q)$ at about 29 nm^{-1} . The values slightly change with Q . As clearly seen in the table, a large difference between the $\Delta_{\text{Pd}}S(Q)$ and $S(Q)$ is realized mainly in $S_{\text{PdPd}}(Q)$, and the others are very small.

III. RESULTS

Figure 1(a) shows the Pd $3d_{5/2}$ core-level PES spectra for the PNCP, PNP, and PCP metallic glasses. For the PNP alloy, the peak locates at about -335.55 eV . By replacing most of the Ni atoms with Cu, the peak shifts toward the deeper binding energy of about -335.95 eV in PNCP. With complete replacement, the peak position returns to a shallower binding energy of -335.60 eV in PCP. Thus, the Pd $3d_{5/2}$ core level of the PCNP alloy is about 0.4 eV deeper than those of the other alloys. Figure 1(b) depicts the Ni $3p$ core spectra of the PNP and PNCP alloys. The spectra comprise the $3p_{3/2}$ and $3p_{1/2}$ contributions at about -66 and -68 eV , respectively. Although the data of the PNCP alloy are rather scattered due to the small Ni concentration, the peaks are slightly shifted by about 0.2 eV. Figure 1(c) exhibits the Cu $3p$ core spectra of the PNCP and PCP glasses, including $3p_{3/2}$ at about -74.5 eV and $3p_{1/2}$ at about -77.0 eV . The PNCP glass has again a deeper binding energy of about 0.2 eV. As a result, all of the metallic elements show deeper core-level binding energies in PNCP. A plausible interpretation is that charge transfer occurs from the metallic elements to the metalloid P atoms causing a shift in the P core levels toward shallower binding energies. However, the present P $2p$ core-level PES measurements demonstrate much more fruitful results.

Figure 2 shows the P $2p$ core spectra of the three glasses. Except some small shoulders, the PNP spectrum is dominated by only one pair of peaks, which can be assigned to the

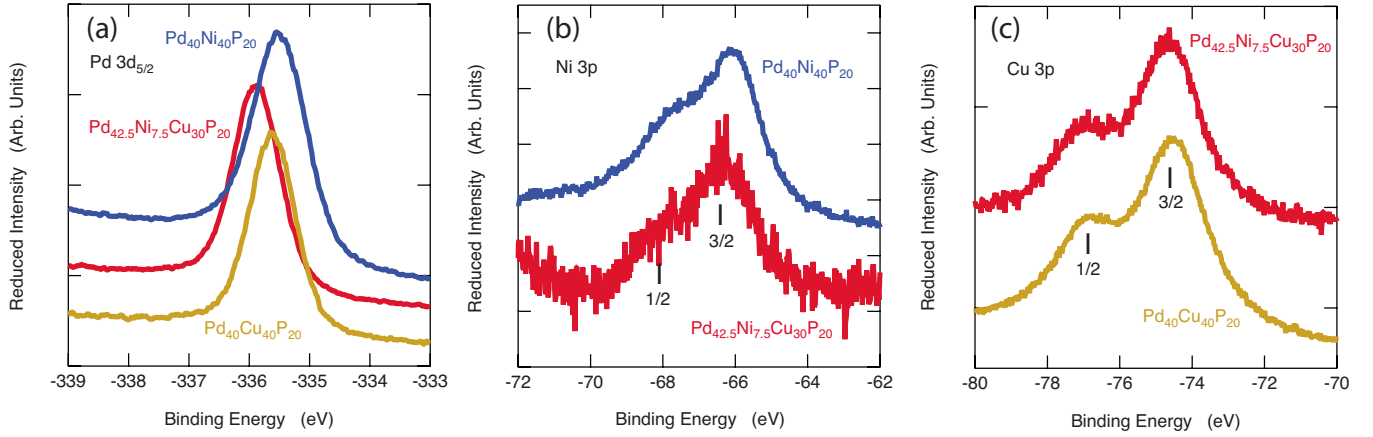


FIG. 1. (Color online) The PES spectra of (a) $\text{Pd } 3d_{5/2}$, (b) $\text{Ni } 3p$, and (c) $\text{Cu } 3p$ core levels for the PNCP, PNP, and PCP.

$2p_{3/2}$ and $2p_{1/2}$ emissions at -129.3 and -130.2 eV, respectively. If Ni is replaced by Cu, an additional pair appears in PNCP spectrum at deeper binding energies, i.e., the $2p_{3/2}$ and $2p_{1/2}$ contributions at -129.8 and -130.7 eV, respectively. Thus there are two energetically different states in the electronic structure of the P atoms in PNCP. By fully replacing Ni with Cu, the intensity of the new P $2p$ pair increases, but the peak positions of the whole spectra shift toward shallower binding energies by about 0.3 eV.

The most important structural result obtained by the present AXS experiment appears in $\Delta_{\text{Pd}}S(Q)$ for PNP, PNCP, and PCP shown in Fig. 3 together with the corresponding total structure factors $S(Q)$. Other partial information on the $\Delta_{\text{Ni}}S(Q)$ and $\Delta_{\text{Cu}}S(Q)$ are given in Fig. 1 of Ref. 18. Although all of the $S(Q)$ spectra look similar, preshoulders are observed at about 19 nm^{-1} in the Cu-containing PCNP and PCP glasses, which is almost invisible in PNP. It should be noted that these preshoulders become much more enhanced in $\Delta_{\text{Pd}}S(Q)$. Since the Pd-related partial correlations dominate $\Delta_{\text{Pd}}S(Q)$ as shown in Table I, it is concluded that the preshoulder originates from the Pd-Pd intermediate-range

correlations.^{18,19} From the Q position of the preshoulder, the Pd-Pd correlation length is estimated to be $2\pi/19 \sim 0.33 \text{ nm}$.

The differential pair-correlation functions $\Delta_{\text{Pd}}g(r)$ were obtained by Fourier transformation of the corresponding $\Delta_{\text{Pd}}S(Q)$. Figure 4 shows the differential radial distribution functions (DRDF) $4\pi r^2 \rho_0 \Delta_{\text{Pd}}g(r)$ around the first peaks for PNCP, PNP, and PCP, ρ_0 being the number density. Due to the wide Q range measured, the truncation errors are very shallow in the DRDF, and appear mainly below 0.20 nm .

IV. DISCUSSION

First, we shall discuss the inhomogeneity of the microstructure in these BMGs. As seen in Fig. 2, the P $2p$ core spectra in these three glasses have two sites, and that with the deeper binding energy grows up by replacing the Ni atoms with the Cu atoms. In order to clarify these spectral features, data fits were performed by using a linear combination of a Gaussian and a Lorentzian for each peak with a standard background. The thin solid and thin dashed curves in Fig. 2 represent the two components with the deeper and shallower binding energies in the P $2p$ core levels, respectively. The

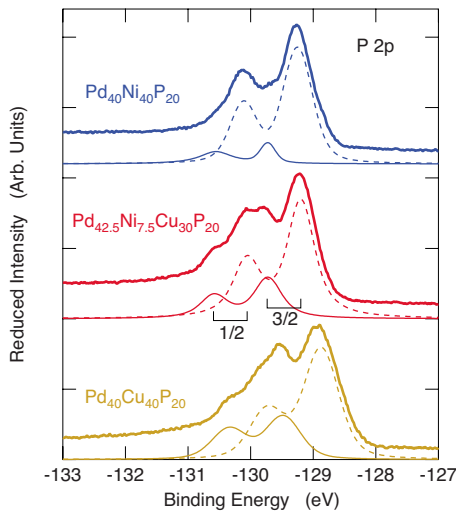


FIG. 2. (Color online) The PES spectra and the fits of the P $2p$ core levels for the PNCP, PNP, and PCP. Thin solid and dashed curves denote two components obtained from the fits.

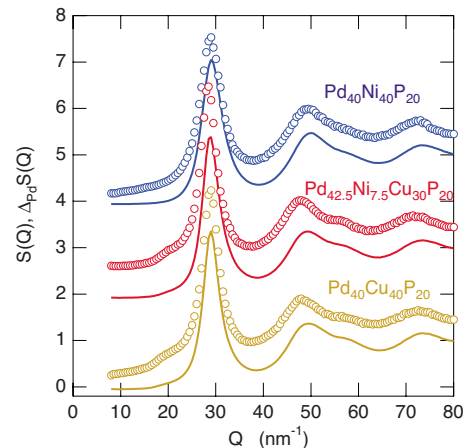


FIG. 3. (Color online) The $\Delta_{\text{Pd}}S(Q)$ (circles) and total $S(Q)$ (solid curves) spectra of PNCP and PNP, and PCP.

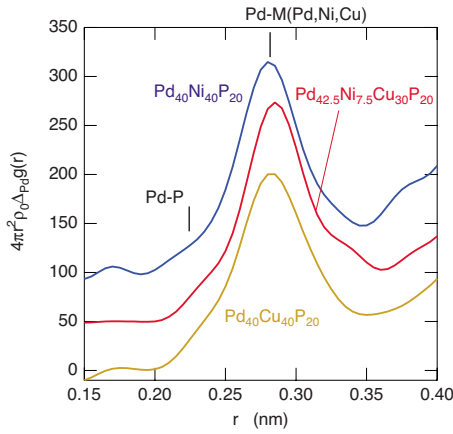


FIG. 4. (Color online) The DRDF spectra close to the Pd K edge around the first peak for the PNCP, PNP, and PCP.

portion of these specific P atoms can be estimated from the area under the P $2p$ core spectra; about 8 % for PNP, about 25 % for PNCP, and about 30 % for PCP. Even in PNP, there is a small portion of the component with deeper binding energy, and it increases with Cu concentration.

It should be noted that the presence of such double P chemical sites is a strong experimental proof for the existence of microscopic elastic inhomogeneity in the PNCP glass, which was proposed by Ichitsubo *et al.*⁷ based on the difference in sound velocities obtained from ultrasonic and IXS measurements. However, the question remains, why the P $2p$ core levels separate into two states in the present BMG systems. A preliminary answer may be obtained from the AXS data,^{18,19} which we have reanalyzed in order to link the electronic and structural features for this paper.

In Fig. 4, the shoulders in the first peak of the DRDFs at about 0.23 nm originate from the Pd-P correlation, which were estimated by Park *et al.*²⁰ for M-P (M: Pd, Ni, or Cu) in PNP and Pd₄₀Ni₁₀Cu₃₀P₂₀ glasses by using their AXS data close to the Ni and Cu K absorption edges and a topological short-range order (TSRO) model using polyhedra clusters. Combined with the Pd-Pd correlation length of about 0.33 nm obtained above, the Pd-Pd bond angle is estimated to be between 85° and 92°, almost a right angle. It should be noted that such a Pd-P-Pd bond with a right angle is not a specific atomic configuration in the polyhedra clusters used for the structural analysis by Park *et al.*,²⁰ i.e., *trigonal prism capped with three half octahedra* or *transformed tetragonal dodecahedron* centered by a P atom.

Since the preshoulders in $\Delta_{\text{Pd}}S(Q)$ are small and highly damped, parts of the P atoms may form such a specific atomic configuration. The areas under the preshoulders are closely correlated with the portion of the new sites appearing in the P $2p$ core levels given in Fig. 2. These P sites are very stable because their $2p$ core levels form new shoulders located at about 0.5 eV lower than the original ones. The formation of such a specific atomic configuration may act like a glue to form a dense random packing configuration of metallic elements.

Second, we shall discuss the excellent GFA of the PNCP glass. Since the PCP glass shows a very poor GFA but has a new P $2p$ core site and a preshoulder in $\Delta_{\text{Pd}}S(Q)$, it is un-

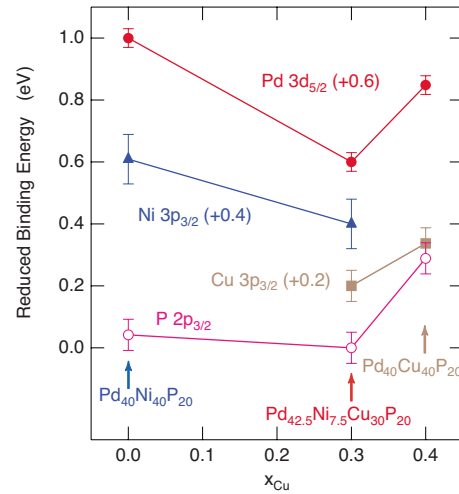


FIG. 5. (Color online) The binding energies of the core levels reduced to the PNCP values.

likely that the existence of the intermediate Pd-P-Pd correlations itself is directly related to the excellent GFA in the PNCP glass as was stated in a previous paper.¹⁹

The energies of the center of gravity of P $2p_{3/2}$ peaks obtained from the fits and reduced by the PNCP value are given in Fig. 5 by the open circles as a function of the Cu concentration. There seems to be a good relation between the GFA and the P $2p_{3/2}$ binding energy. The fitted values of the Pd $3d_{5/2}$, Ni $3p_{3/2}$, and Cu $3p_{3/2}$ peaks are also given by solid circles, triangles, and squares, respectively. It is clearly observed that all of the core levels in PNCP have the deepest binding energies among these glasses, indicating a possibility that the most excellent glass former PNCP has the most stable electronic states.

Core-level PES works were performed by Alamgir *et al.*^{21,22} for Pd_xNi_{80-x}P₂₀, where $x=40$ has the lowest CCR. However, they found an almost linear variation in the P $2p$ core-level energies with x , and constant values for the Pd $3d$ and Ni $2p$ states. We think that charge transfer from the P atoms to the metallic elements with x causes the large core shifts, and hides small core shifts corresponding to the GFA in Pd_xNi_{80-x}P₂₀.

The first peak position in the DRDFs seen in Fig. 4 is at about 0.28 nm, which can be identified as the Pd-M (M: Pd, Ni, or Cu) interatomic distances by the TSRO model.²⁰ A relation between the excellent GFA and the atomic structure of PNCP is that the first peak in DRDF of PNCP shows the longest atomic distance (0.285 nm) among the glasses (0.281 nm for PNP and 0.283 nm for PCP). Similar results were also presented in the previous AXS work with model calculation (Table 2 of Ref. 20), indicating a Pd-M (M: Pd or Ni) distance of 0.268 nm in the PNP glass and 0.280 nm in the Pd_xNi_{80-x}P₂₀ alloy. It is also observed that the first peak of the DRDFs in PNCP shows the highest peak height among the three BMGs (223, 215, and 201 nm⁻¹ for PNCP, PNP and PCP, respectively). The longest and sharpest first-neighbor peak in the DRDF of PNCP may reveal that the Pd sublattice has an atomic configuration with random packing but gathered loosely.

Inoue²³ reviewed the GFA of BMGs from the structural points of view. Based on the previously reported experimen-

tal data, he established that amorphous alloys with a good GFA have (a) atomic configurations with a high degree of dense random packing, (b) new local atomic configurations different from those of the corresponding crystalline phases, and (c) a homogeneous atomic configuration of the multi-components on a long-range scale. The present AXS results on the Pd sublattice may correspond to (a) and (c). What is observed in “(b) the new local atomic configurations” from the present AXS and core-level PES works?

More than a half century ago, Frank²⁴ postulated that there is a significant amount of an icosahedral intermediate-range order in supercooled melts, which consists of compact arrangements of 13 atoms, and possesses a local energy being by 8.4 % smaller than that of dense-packed fcc or hcp structure of the same number of atoms, if atomic interactions are approximated by a Lennard-Jones potential. The existence of the icosahedral clusters has widely been discussed for the metallic glasses as a structural origin of forming stable glassy phases.

Another cluster model for transition-metal-metalloid glassy systems was proposed by Gaskell,^{25,26} which is a trigonal prism capped with three half octahedra centered on the metalloid. This model was an analogy of a metal-metalloid crystal, and its existence in a metallic glass was confirmed by both studies of neutron scattering²⁷ and ¹¹B NMR (Ref. 28) on Ni_{1-x}B_x metallic glasses. A similar crystal analogy for Pd-P-based metallic glasses is a transformed tetragonal dodecahedron centered by a P atom, which was found in Pd₃₀Cu₅₀P₂₀ crystal.²⁹ These two cluster models were discussed for the previous AXS work by Park *et al.*²⁰

In these models, however, a special Pd-P-Pd configuration with a right bond angle found in the present AXS measurement cannot be realized unless a large lattice distortion occurs from them. Nishiyama and Inoue³⁰ reported that the generation and annihilation of a primary Pd₁₅P₂ phase with a diameter of about 15 nm were observed in the supercooled particle sample of Pd₄₀Ni₁₀Cu₃₀P₂₀ having a similar concentration to the PNCP glass. This primary Pd₁₅P₂ crystal has a large lattice parameter, but the P atoms are surrounded by a Pd octahedron, having many Pd-P-Pd configurations with right angle. They discussed that the existence of such a metastable crystal-like cluster in Pd₄₀Ni₁₀Cu₃₀P₂₀ with a large lattice parameter requires a significant change in the local structure of the alloy for the crystallization, and thus lead to the high stability against it.

The present AXS result does support the existence of such a cluster resembling the primary Pd₁₅P₂ crystal in PNCP. However, it is not true that a larger number of the special Pd-P-Pd configurations make the GFA better, which is distinct in the PCP case. As usually discussed in this field, the competition between the stability of the glassy and crystal-

line states is essential to the GFA of metallic glasses. In particular, a steep threshold of the GFA does exist between the PNCP and PCP although the main difference is only the existence of 7.5 at. % of Ni atoms. Thus, a precise determination of the local structures in these glasses is extremely important for the understanding of the mechanism of the excellent GFA of the PNCP glass.

For further structural analysis, however, it is still very difficult to precisely model the local structure of the PNCP glass because information on the P site can hardly be obtained from the AXS experiment due to the small scattering cross section (almost a half of Ni and Cu, and one third of Pd) and the very low energy of the *K* absorption edge (2149 eV) of the P element compared to the other transition metals. On the other hand, neutron scattering may be a good tool to investigate the local structure around the P atoms since the neutron-scattering length of P is comparable to those of the other transition metals. Also, an XAFS experiment becomes nowadays possible to perform close to such a low x-ray energy of P *K* edge. After obtaining the local structure around the P atoms by these methods, we will construct a much more reliable atomic configuration model with the help of a reverse Monte Carlo modeling analysis.

V. CONCLUSION

In order to find experimental evidence for the inhomogeneity in the excellent PNCP BMG, core-level PES and AXS measurements were performed, and the results were compared to those in PNP and PCP. The P 2*p* core levels clearly separate into two states, indicating that the P atoms have two different chemical sites, which is a strong experimental proof for the existence of the elastic inhomogeneity. From the AXS close to the Pd *K* edge, a special Pd-P-Pd atomic configuration was observed, which is related to the stable site in the P 2*p* core levels. All of the core levels measured in PNCP have the deepest binding energies among these glasses, indicating the most stable electronic states. Local structure around the P atoms is discussed by the AXS data and a metastable crystal appeared in a supercooled Pd₄₀Ni₁₀Cu₃₀P₂₀.

ACKNOWLEDGMENTS

T.I., E.M., and N.N. acknowledge financial support by Grant-in-Aid for Scientific Research on the Priority Area Investigation of “Materials Science of Bulk Metallic Glasses” from the Ministry of Education, Culture, Sports, Science, and Technology of Japan. The PES experiments were carried out at BL7 of the HiSOR (Proposal No. 06A51 and 07A36), and the AXS experiments were performed at BM02 of the ESRF (Proposal No. ME1002 and HD162).

*hosokawa@cc.it-hiroshima.ac.jp

- ¹P. G. Debenedetti and F. H. Stillinger, *Nature (London)* **410**, 259 (2001).
- ²T. Scopigno, G. Ruocco, and F. Sette, *Rev. Mod. Phys.* **77**, 881 (2005).
- ³U. Balucani and M. Zoppi, *Dynamics of the Liquid State* (Clarendon, Oxford, 1994).
- ⁴S. H. Chong, *Phys. Rev. E* **74**, 031205 (2006).
- ⁵T. Scopigno, U. Balucani, G. Ruocco, and F. Sette, *Physica B* **318**, 341 (2002).
- ⁶B. Ruzicka, T. Scopigno, S. Caponi, A. Fontana, O. Pilla, P. Giura, G. Monaco, E. Pontecorvo, G. Ruocco, and F. Sette, *Phys. Rev. B* **69**, 100201(R) (2004).
- ⁷T. Ichitsubo, S. Hosokawa, K. Matsuda, E. Matsubara, N. Nishiyama, S. Tsutsui, and A. Q. R. Baron, *Phys. Rev. B* **76**, 140201(R) (2007).
- ⁸T. Ichitsubo, E. Matsubara, K. Miyagi, W. Itaka, K. Tanaka, and S. Hosokawa, *Phys. Rev. B* **78**, 052202 (2008).
- ⁹T. Ichitsubo, E. Matsubara, T. Yamamoto, H. S. Chen, N. Nishiyama, J. Saida, and K. Anazawa, *Phys. Rev. Lett.* **95**, 245501 (2005).
- ¹⁰W. Schirmacher, *Europhys. Lett.* **73**, 892 (2006).
- ¹¹W. Schirmacher, G. Ruocco, and T. Scopigno, *Phys. Rev. Lett.* **98**, 025501 (2007).
- ¹²N. Nishiyama and A. Inoue, *Mater. Trans., JIM* **37**, 1531 (1996).
- ¹³N. Nishiyama and A. Inoue, *Appl. Phys. Lett.* **80**, 568 (2002).
- ¹⁴H. W. Kui and D. Turnbull, *Appl. Phys. Lett.* **47**, 796 (1985).
- ¹⁵M. Taniguchi and J. Ghijsen, *J. Synchrotron Radiat.* **5**, 1176 (1998).
- ¹⁶*Synchrotron Radiation Instrumentation*, Ninth International Conference on Synchrotron Radiation Instrumentation, edited by J.-Y. Choi and S. Rah, AIP Conf. Proc. No. 879 (AIP, New York, 2007), p. 1743.
- ¹⁷S. Hosokawa, Y. Wang, J.-F. Bézar, J. Greif, W.-C. Pilgrim, and K. Murase, *Z. Phys. Chem.* **216**, 1219 (2002).
- ¹⁸S. Hosokawa, J.-F. Bézar, N. Boudet, T. Ichitsubo, E. Matsubara, and N. Nishiyama, *J. Phys.: Conf. Ser.* **144**, 012055 (2009).
- ¹⁹S. Hosokawa, J.-F. Bézar, N. Boudet, T. Ichitsubo, E. Matsubara, and N. Nishiyama, *Mater. Trans.* **48**, 2358 (2007).
- ²⁰C. Park, M. Saito, Y. Waseda, N. Nishiyama, and A. Inoue, *Mater. Trans., JIM* **40**, 491 (1999).
- ²¹F. M. Alamgir, H. Jain, A. C. Miller, D. B. Williams, and R. B. Schwarz, *Philos. Mag. B* **79**, 239 (1999).
- ²²F. M. Alamgir, H. Jain, R. B. Schwarz, O. Jin, and D. B. Williams, *J. Non-Cryst. Solids* **274**, 289 (2000).
- ²³A. Inoue, *Acta Mater.* **48**, 279 (2000).
- ²⁴F. C. Frank, *Proc. R. Soc. London, Ser. A* **215**, 43 (1952).
- ²⁵P. H. Gaskell, *J. Non-Cryst. Solids* **32**, 207 (1979).
- ²⁶P. H. Gaskell, *J. Non-Cryst. Solids* **75**, 329 (1985).
- ²⁷K. Suzuki, T. Fukunaga, F. Itoh, and N. Watanabe, in *Rapidly Quenched Metals*, edited by S. Steeb and H. Warlimont (Elsevier, Amsterdam, 1985), p. 479.
- ²⁸P. Panissod, I. Bakonyi, and R. Hasegawa, *Phys. Rev. B* **28**, 2374 (1983).
- ²⁹M. El-Boragy, M. Ellner, and K. Schubert, *Z. Metallkd.* **75**, 302 (1984).
- ³⁰N. Nishiyama and A. Inoue, *Mater. Sci. Forum* **386-388**, 105 (2002).